Peertechz

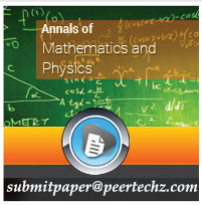

MATHEMATICS AND PHYSICS GROUP

ANNALS OF Mathematics and Physics OPEN ACCESS JOURNAL

ISSN: 2689-7636 DOI: https://dx.doi.org/10.17352/amp

Research Article

Asymmetry in Spectral Graph Theory: Harmonic Analysis on Directed Networks via Biorthogonal Bases

Chandrasekhar Gokavarapu*

Department of Mathematics, Government College, Rajahmundry, Andhra Pradesh, India

Submitted : 29 December, 2025
Accepted : 12 January, 2026
Published : 13 January, 2026

***Corresponding author:** Chandrasekhar Gokavarapu, Department of Mathematics, Government College, Rajahmundry, Andhra Pradesh, India,
E-mail: chandrasekhargokavarapu@gmail.com

Keywords: Directed graphs; Random walks; Non-normal matrices; Biorthogonal eigenvectors; Graph Fourier transform; Sampling; Reversibility

https://www.mathematicsgroup.us

Check for updates

Abstract

The operator-theoretic dichotomy underlying diffusion on directed networks is symmetry versus non-self-adjointness of the Markov transition operator. In the reversible (detailedbalance) regime, a directed random walk P is self-adjoint in a stationary π-weighted inner product and admits orthogonal spectral coordinates; outside reversibility, P is genuinely non-self-adjoint (often non-normal), and stability is governed by biorthogonal geometry and eigenvector conditioning. In this paper, we develop an original harmonic-analysis framework for directed graphs anchored on the random-walk transition matrix $P = D_{out}^{-1}A$ and the random-walk Laplacian $L_{rw} = I-P$. Using biorthogonal left/right eigenvectors, we define a Biorthogonal Graph Fourier Transform (BGFT) adapted to directed diffusion, propose a diffusion-consistent frequency ordering based on decay rates $R(1-\lambda)$, and derive operator norm stability bounds for iterated diffusion and for BGFT spectral filters. We prove sampling and reconstruction theorems for P-bandlimited (equivalently L_{rw}-bandlimited) signals and quantify noise amplification through the conditioning of the biorthogonal eigenbasis. A simulation protocol on directed cycles and perturbed non-normal digraphs demonstrates that asymmetry alone does not dictate instability, whereas non-normality and eigenvector illconditioning drive reconstruction sensitivity, making BGFT the correct analytical language for directed diffusion processes.

2020 Mathematics Subject Classification: Primary 05C50; Secondary 15A18, 47A10, 60 J10, 94A12.

1. Introduction

1.1 Symmetry *vs.* non-self-adjointness: Markov operators on directed networks

A directed network naturally carries a one-step evolution operator: the random-walk (Markov) transition matrix

$$P = D_{out}^{-1} A,\ P1 = 1,$$

and its generator $L_{rw} = I-P$. From the operator-theoretic viewpoint, the central dichotomy is not "directed vs. undirected" per se, but symmetry vs. non-self-adjointness of the Markov operator.

The symmetry regime is the reversible (detailed-balance) case: there exists a stationary distribution π with $\Pi = \mathrm{diag}(\pi)$ such that

$$\Pi P = P^{\top}\Pi,$$

equivalently, P is self-adjoint in the weighted Hilbert space $(\mathbb{C}^n, \langle .\ ,\ . \rangle_\pi)$. In that regime, P is similar to a symmetric matrix $S = \Pi^{1/2} P \Pi^{-1/2}$, hence the spectrum is real, and there is an orthonormal eigenbasis in the π-metric. This is precisely the mechanism by which a directed diffusion can retain symmetry (in a stationary metric), recovering Parseval-type identities and a clean variational frequency ordering. The asymmetry regime is non-reversibility, where P is genuinely non-self-adjoint and may be non-normal; then orthogonality is lost, spectral coordinates can be ill-conditioned, and stability is governed by eigenvector conditioning and non-normal effects [1-3].

Our goal is to build a harmonic-analysis calculus that is native to the Markov operator P: it should reduce to the classical orthogonal theory in the reversible (symmetric)

Citation: Gokavarapu C. Asymmetry in Spectral Graph Theory: Harmonic Analysis on Directed Networks via Biorthogonal Bases. Ann Math Phys. 2026;9(1):001-006. Available from: https://dx.doi.org/10.17352/amp.000174

regime, and it should remain exact and analyzable in the non-reversible (non-self-adjoint) regime. The correct language here is biorthogonality: left/right eigenvectors provide an exact analysis/synthesis pair even when P is not normal.

1.2 Position relative to the graph: Fourier analysis

Graph Fourier analysis is often introduced through symmetric operators (undirected Laplacians/adjacencies), which guarantee orthogonal eigenvectors and stable spectral coordinates [4-7]. Directed graph settings typically replace symmetry by alternative constructions: optimization-based directed transforms that seek to minimize a directed variation [8], or transforms based on the Jordan decomposition of the adjacency matrix A [6]. While these approaches provide powerful tools for signal compression, they often decouple the transform from the underlying physics of diffusion. Our approach is complementary and more "operator first": we start from the canonical diffusion operator P and develop an exact biorthogonal Fourier calculus for directed diffusion, with a transparent symmetry/asymmetry interpretation in terms of reversibility [9,10]. Unlike methods that force orthogonality through isometric embeddings, our BGFT embraces the biorthogonal geometry inherent in non-reversible Markov chains.

1.3 Main contributions

Main contributions (original):

1. **(Markov-operator BGFT)** We define the Biorthogonal Graph Fourier Transform (BGFT) for the random-walk operator P (equivalently, $L_{rw} = I - P$) via left/right eigenvectors, yielding exact analysis/synthesis identities and diagonal dynamics for diffusion iterates.

2. **(Symmetry principle via reversibility)** We identify reversibility (detailed balance) as the precise symmetry notion for directed diffusion: in the π-metric, reversible P becomes selfadjoint, restoring orthogonality/Parseval identities and an exact diffusion-variational frequency ordering.

3. **(Diffusion-consistent frequency)** We propose a diffusion-consistent frequency ordering based on the decay rate $\Re(1-\lambda)$ (and magnitude alternatives), aligning with the symmetry limit and the long-time behavior of $x_{t+1} = Px_t$.

4. **(Stability theorems for non-self-adjoint diffusion)** We prove operator-norm bounds for diffusion iterates P^t and for BGFT spectral filters $h(P)$, explicitly separating eigenvalue decay from eigenvector conditioning, the key instability driver in non-normal settings.

5. **(Sampling and reconstruction)** We prove sampling/reconstruction theorems for P bandlimited signals and quantify noise amplification through $\sigma_{\min}(P_M V_\Omega)$ and conditioning of the biorthogonal eigenbasis.

6. **(Asymmetry *vs.* non-normality: numerical separation)** We introduce simple indices for directedness and departure from normality and provide experiments (directed cycle *vs.* perturbed non-normal digraphs) showing that asymmetry alone need not cause instability, whereas non-normality and eigenvector ill-conditioning do.

1.4 Organization

Section 2 introduces directed diffusion operators and asymmetry/non-normality indices. Section 3 presents reversibility as the symmetry regime in the stationary metric. Sections 4-5 develop BGFT and stability bounds for diffusion and filtering. Section 6 presents sampling and reconstruction results, followed by algorithms and illustrative experiments.

2. Preliminaries: directed diffusion operators

2.1 Directed graphs, adjacency, and out-degree

Let $G = (V, E, w)$ be a directed weighted graph with $|V| = n$ and adjacency $A \in \mathrm{R}^{n\times n}$:

$$A_{ij} = \begin{cases} w(i,j), & (i,j) \in E \\ 0, & otherwise \end{cases}$$

Define out-degrees d^{out}_i

$= \mathrm{P}_j A_{ij}$ *and* $D_{out} = \mathrm{diag}\left(d_1^{out},\ldots,d_n^{out}\right)$.

2.2 Transition matrix and random-walk Laplacian

Definition 2.1 (Random-walk transition matrix). Assume $d^{\text{out}}_i > 0$ for all i (no sinks). Define

$P := D_{\text{out}}^{-1} A.$

Then P is row-stochastic: $P\mathbf{1} = \mathbf{1}$.

Definition 2.2 (Random-walk Laplacian). Define

$L_{rw} = I - P$

Proposition 2.3 (Basic properties). (i) $P\mathbf{1} = \mathbf{1}$ and $L_{rw}\mathbf{1} = 0$. (ii) If P is irreducible and aperiodic, then the diffusion $x_{t+1} = Px_t$ converges to the stationary component (Markov mixing perspective).

Proof. (i) Row-stochasticity gives $P\mathbf{1} = \mathbf{1}$, hence $(I - P)\mathbf{1} = 0$.

(ii) This is standard Markov chain theory; see [2,9,10].

2.3 Asymmetry and non-normality indices

Definition 2.4 (Asymmetry index). For any matrix M, define $a(M) := \| M - M^\top \|_F / \| M \|_F$ (with $a(0) = 0$).

Definition 2.5 (Departure from normality). For any matrix M, define $\delta(M) := \| MM^* - M^*M \|_F / \| M \|_F^2$ (with $\delta(0) = 0$).

Such non-normality measures (and related bounds) are classical in matrix analysis; see [3,11-14].

We will use these for $M = P$ and $M = L_{rw}$ to separate structural directedness from numerical instability drivers.

Citation: Gokavarapu C. Asymmetry in Spectral Graph Theory: Harmonic Analysis on Directed Networks via Biorthogonal Bases. Ann Math Phys. 2026;9(1):001-006. Available from: https://dx.doi.org/10.17352/amp.000174

3. Reversibility as the symmetry regime for directed diffusion

Let $P \in R^{n\times n}$ be row-stochastic ($P\mathbf{1} = \mathbf{1}$). Assume P has a stationary distribution $\pi \in R^n$ with $\pi_i > 0$ $\pi^\top P = \pi^\top$. Let $\Pi := \mathrm{diag}(\pi)$.

Define the π-weighted inner product and norm by

$$\langle x, y\rangle_\pi := x^\top \Pi y \,\|\, x\|_\pi^2 := \langle x, y\rangle_\pi$$

The adjoint of P with respect to $\langle\cdot,\cdot\rangle_\pi$ is

$$P^\dagger := \Pi^{-1} P^\top \Pi, \text{ so that } \langle Px, y\rangle_\pi = x, P^\dagger y_\pi$$

Definition 3.1 (Reversibility / detailed balance). P is reversible (w.r.t. π) if

$$\Pi P = P^\top \Pi, \quad \text{equivalently}, P = P\dagger.$$

This detailed-balance condition is standard in reversible Markov chain theory; see [2,9,15].

Theorem 3.2 (Weighted symmetry equivalences). The following are equivalent:

(i) P is reversible $\Pi P = P^\top \Pi$.

(ii) P is self-adjoint in $\langle .\,,.\rangle_\pi$: $P = P^\dagger$.

(iii) The similarity transform $S := \Pi^{1/2} P \Pi^{-1/2}$. is symmetric: $S = S^\top$.

In this case, P has a complete -orthonormal eigenbasis, and all eigenvalues are real.

Proof. (i) ⇔ (ii) is the definition of $P^\dagger$. For (i) ⇒ (iii), multiply $\Pi P = P^\top \Pi$ on the left by $\Pi^{-1/2}$ and on the right by $\Pi^{-1/2}$ to get $\Pi^{1/2} P \Pi^{-1/2} = (\Pi^{1/2} P \Pi^{-1/2})^\top$. Conversely, (iii) ⇒ (i) follows by reversing the steps. If S is symmetric, it is orthogonally diagonalizable with real eigenvalues, hence so is P by similarity.

See also [9,10] for related equivalences and consequences.

Remark 3.3 (Symmetry/asymmetry interpretation for this paper). Undirected diffusion is symmetric in the standard Euclidean inner product. Directed diffusion can still be symmetric in the weighted π-inner product exactly in the reversible regime. Non-reversibility is the correct notion of asymmetry for random-walk harmonic analysis.

4. Biorthogonal Graph Fourier Transform (BGFT) for randomwalk diffusion

4.1 Left/right eigenvectors and BGFT

Assumption 4.1 (Diagonalizability). *Assume P is diagonalizable over C*:

$$P = V\Lambda V^{-1}, \ \Lambda = \mathrm{diag}(\lambda_1,\ldots,\lambda_n),$$

with right eigenvectors $V = [v_1 \cdots v_n]$.

Remark 4.2 (Non-diagonalizable operators). While Assumption 4.1 holds for almost all transition matrices (diagonalizable matrices are dense in $C^{n\times n}$), certain highly symmetric digraph structures can yield non-diagonalizable P. In such cases, the BGFT can be generalized using the Jordan canonical form or the Schur decomposition. However, the biorthogonal framework presented here focuses on the most common case where a complete set of eigenvectors exists, providing a direct physical link to decay modes.

Definition 4.3 (BGFT (diffusion version)). For a graph signal $x \in C^n$, define BGFT coefficients

$$x\mathrm{b} := U^* X, \ x\mathrm{b}_k = u^* kX \tag{1}$$

and synthesis

$$x = V\hat{x} = \sum_{k=1}^{n} v_k \hat{x}_k \tag{2}$$

Theorem 4.4 (Perfect reconstruction). Under Assumption 4.1, for all $x \in C^n$,

$$I = \mathrm{X} vku^* k, \quad x = \mathrm{X} vku^* kX$$

Proof. Since $U^*V = I$, we have $VU^* = I$; expand VU^* in columns/rows.

4.2 Diffusion dynamics are diagonal in BGFT coordinates

Theorem 4.5 (BGFT-domain diffusion). *Let $x_{t+1} = Px_t$ with $x_0 \in C^n$. Then*

$$xbt = U_* X_t = \Lambda tx\,\mathrm{b}0, \ xt = V\Lambda_t U_{*X0}$$

Equivalently, for $L_{rw} = I - P$,

$$(\widehat{L_{rw}x}) = (I - \Lambda)\hat{x}\,.$$

Proof. Use $P = V \Lambda U^*$ and $U^*V = I$. Then $U^*(Px) = \Lambda(U^*x)$ and iterate.

4.3 Diffusion-consistent frequency ordering

For diffusion, the mode with eigenvalue λ evolves as λ^t. If $|\lambda| < 1$, it decays; if $\lambda \approx 1$, it is slowly varying (low frequency). We define the diffusion decay rate:

$$\omega_{diff}(\lambda) := \Re(1 - \lambda).$$

Low ω_{diff} corresponds to persistent/slow modes; high ω_{diff} corresponds to fast decay. Compared to the imaginary-part ordering (phase) often used in adjacency-based GFTs, $\Re(1 - \lambda)$ provides a direct measure of spectral energy dissipation. This choice aligns with the variational property of the random-walk Laplacian, where $\Re(1 - \lambda)$ quantifies the smoothness of a mode relative to the one-step diffusion process.

5. Directed diffusion filtering and stability bounds

5.1 Spectral filters

Definition 5.1 (BGFT spectral filter for diffusion). Let h: C → C. Define

$$H := Vh(\Lambda)U^*.$$

Proposition 5.2 (Diagonal action in BGFT domain). For $x = U^*x$, b

Citation: Gokavarapu C. Asymmetry in Spectral Graph Theory: Harmonic Analysis on Directed Networks via Biorthogonal Bases. Ann Math Phys. 2026;9(1):001-006. Available from: https://dx.doi.org/10.17352/amp.000174

$$Hx_{\mathrm{d}} = U^{*}Hx = h(\Lambda)x.\mathrm{b}\ \textit{Proof}.\ \textit{Compute}\ U^{*}Vh(\Lambda)U^{*}x = h(\Lambda)x.$$

5.2 Operator-norm stability: diffusion and filtering

Theorem 5.3 (Norm bound for diffusion iterates). Assume $P = V\Lambda V^{-1}$. *Then for every* $t \in \mathrm{N}$,

$$P^{t}_{k\,2} \le \mathrm{cond}(V)\max\left|\lambda_{k}\right|^{t},\ \mathrm{cond}($$

Proof. $P^{t} = V\Lambda^{t}V^{-1}$, hence

$$P^{t}{}_{2} \le \|V\|_{2}\ \Lambda^{t}{}_{2}V^{-1}{}_{2} = \mathrm{cond}(V)\max_{k}\left|\lambda_{k}\right|^{t}.$$

Theorem 5.4 (Norm bound for spectral filters). *Let* $H = Vh(\Lambda)V^{-1}$. *Then* $\|H\|_{2} \le$

$$\mathrm{cond}(V)\max\left|h\left(\lambda_{k}\right)\right|.$$

Proof. $\|H\|_{2} \le \|V\|_{2}\|h(\Lambda)\|_{2}\ V^{-1}{}_{2} = \mathrm{cond}(V)\max_{k}\left|h\left(\lambda_{k}\right)\right|$.

Remark 5.5 (Symmetry/asymmetry and Instability). When P is normal and diagonalizable by a unitary basis, cond(V) = 1, and the bounds become tight and symmetry-like. It is critical to distinguish between structural asymmetry ($a(P) > 0$) and numerical instability (cond(V) $\gg 1$). Asymmetry is a prerequisite for the loss of orthogonality, but it does not necessitate instability; for instance, the directed cycle is maximally asymmetric but remains normal and perfectly stable. For non-normal P, cond(V) can be large, creating instability even if $|\lambda_{k}| \le 1$. Our numerical experiments in Section 9 confirm that this ill-conditioning, rather than directedness per se, drives the reconstruction error.

6. BGFT energy in the stationary metric and its symmetry limit

Assume P is diagonalizable over C: $P = V\Lambda V^{-1}$ and define $U^{*} := V^{-1}$. Let $x_{\mathrm{b}} := U^{*}x$ be BGFT coefficients so that $x = Vx$.

Theorem 6.1 (π-metric Parseval identity). For any $x \in \mathrm{C}^{n}$,

$$\|x\|_{\pi}^{2} = \hat{x}^{*}G_{\pi}\hat{x},\ G_{\pi} := V^{*}\Pi V$$

Proof. Since $x = Vx\mathrm{b}, \|x\|^{2}{}_{\pi} = x^{*}\Pi x = x\mathrm{b}^{*}(V^{*}\Pi V)x\mathrm{b}$.

Corollary 6.2 (Two-sided bounds via conditioning in π). Let $W := \Pi 1/2V$. Then

$$\sigma_{\min}(W)^{2}\ \|\hat{x}\|_{2}^{2} \le \|x\|_{\pi}^{2} \le \sigma_{\max}(W)^{2}\ \|\hat{x}\|_{2}^{2}$$

Equivalently, energy distortion is controlled by $\kappa(W) = \sigma_{\max}(W)/\sigma_{\min}(W)$.

6.1 Diffusion variation and frequency ordering

Define the random-walk Laplacian $L_{\mathrm{rw}} := I - P$ and the diffusion variation

$$\mathrm{TV}_{\pi}(x) := L_{\mathrm{rw}}x_{\pi}^{2} = \|(I-P)x\|_{\pi}^{2}$$

Theorem 6.3 (BGFT-domain bounds for diffusion variation). *With* $x = Vx$ *and* $W = \Pi^{1/2}V$, b *n n*

$$\sigma_{\min}(W)_{2}\mathrm{X}\left|1-\lambda_{k}\right|2\,|\,x\mathrm{b}k\,|\,2 \le \mathrm{TV}\pi(x) \le \sigma_{\max}(W)_{2}\mathrm{X}\left|1-\lambda_{k}\right|2\,|\,x\mathrm{b}k\,|\,2$$

Proof. $(I-P)x = V(I-\Lambda)x\mathrm{b}$.

Then $\|(I-P)x\|_{\pi} = \Pi^{1/2}V(I-\Lambda)x\mathrm{b}_{2} = \|W(I-\Lambda)x\mathrm{b}\|_{2}$. Apply $\sigma_{\min}(W)\|z\|_{2} \le \|Wz\|_{2} \le \sigma_{\max}(W)\|z\|_{2}$ to $z = (I-\Lambda)x\mathrm{b}$ and square.

Remark 6.4 (Exact symmetry limit). If P is reversible, one can choose $V\pi$-orthonormal, hence $W = \Pi^{1/2}V$ is unitary and $\sigma_{\min}(W) = \sigma_{\max}(W) = 1$. Then the inequalities become equalities, and $|1 - \lambda_{k}|$ becomes an exact diffusion frequency.

7. Sampling and reconstruction for diffusion-bandlimited signals

Let $\Omega \subset \{1,\ldots,n\}$ with $|\Omega| = K$ represent the "low diffusion-frequency" modes (e.g. smallest $\omega_{\mathrm{diff}}(\lambda)$ or largest $\Re(\lambda)$). Let $V_{\Omega} \in \mathrm{C}^{n\times K}$ contain $\{v_{k}\}_{k\in\Omega}$.

Definition 7.1 (Diffusion-bandlimited signals). A signal x is Ω-bandlimited (relative to P) if $x = V_{\Omega}c$ for some $c \in \mathrm{C}^{K}$.

Bandlimited sampling on graphs has a substantial literature; see, e.g., [16-18]. Let $M \subset V$, $|M| = m$, and $P_{M} \in \{0,1\}^{m\times n}$ be the restriction operator.

Theorem 7.2 (Exact recovery). If $x = V_{\Omega}c$ and $P_{M}V_{\Omega}$ has full column rank K, then x is uniquely determined by samples $y = P_{M}x$ and recovered by

$$\mathrm{b}c = \left(P_{M}V_{\dot{\mathrm{U}}}\right)^{\dagger}y, x\mathrm{b} = V_{\dot{\mathrm{U}}}\mathrm{b}c$$

Proof. Full column rank makes $P_{M}V_{\Omega}$ injective; solve the linear system in least squares. Related sampling-set conditions and reconstruction stability on graphs are discussed in [16-19].

Theorem 7.3 (Noise sensitivity). If $y = P_{M}x + \eta$, *then the least-squares reconstruction satisfies.*

$$\|\hat{x} - x\|_{2} \le V_{\Omega 2}\left(P_{M}V_{\Omega}\right)^{\dagger}{}_{2}\,\|\eta\|_{2} = V_{\Omega 2}\frac{\|\eta\|_{2}}{\sigma_{\min}\left(P_{M}V_{\Omega}\right)}$$

Proof. b $c - c = (P_{M}V_{\Omega})^{\dagger}\eta$ and $x_{\mathrm{b}} - x = V_{\Omega}(_{\mathrm{b}}c - c)$.

8. Algorithms

Algorithm 1 BGFT for random-walk diffusion

Require: A (directed adjacency), D_{out} invertible, signal x

Ensure: BGFT coefficients x, eigenpairs (Λ, V)

1: P← $D_{out}^{-1}A$, $\mathrm{L}_{\mathrm{rw}\leftarrow}$ I-P

2: Compute eigendecomposition P = $V\ \Lambda\ V^{-1}$ (complex arithmetic)

3: U*$_{\leftarrow}$ V-1

4: x $_{\leftarrow}$ U* xb

5: return (x,Λ,V) b

Algorithm 2: Diffusion filtering and bandlimited reconstruction

Citation: Gokavarapu C. Asymmetry in Spectral Graph Theory: Harmonic Analysis on Directed Networks via Biorthogonal Bases. Ann Math Phys. 2026;9(1):001-006. Available from: https://dx.doi.org/10.17352/amp.000174

Table 1: Minimal numerical illustration for the transition-operator BGFT.

Graph	$\alpha(P)$	$\delta(P)$	$\kappa(V)$	$\kappa(P_M V_\Omega)$	RelErr
Undirected cycle A_{und}	0	0	1.2453204511204569	36.59492056037454	0.0000031215500108761767
Directed cycle $A_{\vec{}}$	1.4142135623730951	0	1	93.04681515171424	0.00000708090322451635 3
Perturbed A_ε ($\varepsilon = 0$)	1.414213562373095	0.02987165083714049	28.011585066632986	352.8935063092261	0.0000252391408392986 2

Require: $P = V \Lambda V^{-1}$, response $h(\cdot)$, bandlimit Ω, sample set M, samples y **Ensure:** filtered signal Hx or reconstructed x

1: **Filtering:** $H \leftarrow V\, h(\Lambda) V^{-1}$, output $Hx \leftarrow Hx$

2: **Reconstruction:** form V_Ω, solve $bc \leftarrow \operatorname{argmin}_c \| \mathrm{PMVWc} - \mathrm{y} \|_2^2$

3: $\hat{x} \leftarrow V \Omega \hat{c}$

9. Experiments: directed cycle vs perturbed non-normal digraphs

9.1 Graphs

Use $n \in \{32,64,128\}$ and compare: (Table 1 above).

1. Undirected cycle C_n (convert to diffusion by symmetrizing and normalizing).

Directed cycle $\overrightarrow{C_n}$: P is a permutation shift (asymmetric but normal/unitary).

Perturbed directed cycle $\overrightarrow{C_n}(\varepsilon)$: add a directed chord, then renormalize rows to keep P stochastic; this typically yields non-normal P and large cond (V).

9.2 Tasks and metrics

- **Diffusion filtering:** low-pass via $h(\lambda) = \exp(-\tau(1 - \lambda))$ (BGFT-defined), compare smoothing strength on the three graphs.
- **Forecasting:** iterate diffusion $x_{t+1} = Px_t$ and compare $\| x_t \|_2$ trends with Theorem 5.3.
- **Sampling/reconstruction:** generate Ω-bandlimited signals and recover from m samples; report RelErr and $\sigma_{\min}(P_M V_\Omega)$.

Perturbed directed cycle $\overrightarrow{C_n}(\varepsilon)$: add a directed chord from node 0 to node $n/2$ with weight $\varepsilon = 20$, then renormalize rows to keep P stochastic; this typically yields non-normal P and large cond (V).

Report tables/figures:

$$\alpha(P), \delta(P), \mathrm{cond}(V), \mathrm{cond}\left(P_M V_{\dot{U}}\right), \mathrm{RelErr} = \frac{\| \hat{x} - x \|_2}{\| x \|_2}$$

Observed separation. The directed cycle is asymmetric ($\alpha(P) > 0$) but normal ($\delta(P) = 0$) with a well-conditioned eigenbasis ($\kappa(V) = 1$), whereas the perturbed digraph remains asymmetric but becomes non-normal ($\delta(P) > 0$) and strongly ill-conditioned ($\kappa(V) \gg 1$), leading to markedly larger reconstruction error, consistent with the stability bounds.

Conclusion

We developed an original diffusion-centered harmonic analysis for directed graphs using the random-walk transition matrix P and Laplacian $L_{\mathrm{rw}} = I - P$. The BGFT provides exact analysis/synthesis, diagonalizes diffusion dynamics, motivates a diffusion-consistent frequency ordering, and yields explicit stability bounds for iterated diffusion and spectral filtering governed by eigenvector conditioning. Sampling and reconstruction theorems quantify how non-normality amplifies noise through $\sigma_{\min}(P_M V_\Omega)$ and cond(V). This establishes a principled symmetry/asymmetry narrative: symmetry yields orthogonality and stability; asymmetry forces biorthogonal geometry; non-normality determines practical robustness.

Acknowledgements

The author expresses his gratitude to the Commissioner of Collegiate Education (CCE), Government of Andhra Pradesh, and the Principal, Government College (Autonomous), Rajahmundry, for continued support and encouragement.

Author contributions

The author is solely responsible for conceptualization, methodology, analysis, software, validation, and writing.

Data availability statement

No external datasets were used. The code that generates the reported numerical table/figures will be provided as a reproducible script and (upon acceptance) via a public repository link.

Appendix

References

1. Chung F. Laplacians and the Cheeger inequality for directed graphs. Annals of Combinatorics. 2005;9(1):1–19. Available from: https://link.springer.com/article/10.1007/s00026-005-0237-z
2. Shuman DI, Narang SK, Frossard P, Ortega A, Vandergheynst P. The emerging field of signal processing on graphs: Extending high-dimensional data analysis to networks and other irregular domains. IEEE Signal Processing Magazine. 2013;30(3):83–98.Availablefrom:https://ieeexplore.ieee.org/document/6494675
3. Sandryhaila A, Moura JMF. Discrete signal processing on graphs: Frequency analysis.IEEETransactionsonSignalProcessing.2014;62(12):3042–3054.Available from: https://ieeexplore.ieee.org/document/6808520
4. Sardellitti S, Barbarossa S, Di Lorenzo P. On the graph Fourier transform for directed graphs. IEEE Journal of Selected Topics in Signal Processing. 2017;11(6):796–811. Available from: https://ieeexplore.ieee.org/document/7979496
5. Marques AG, Segarra S, Mateos G. Signal processing on directed graphs. arXiv [Internet]. 2020. Available from: https://arxiv.org/abs/2008.00586
6. Levin DA, Peres Y. Markov chains and mixing times. 2nd ed. Providence (RI): AmericanMathematicalSociety;2017.Availablefrom:https://pages.uoregon.edu/dlevin/MARKOV/markovmixing.pdf
7. TrefethenLN,EmbreeM.Spectraandpseudospectra:Thebehaviorofnonnormal matricesandoperators.Princeton(NJ):PrincetonUniversityPress;2005.Available from:https://www.karlin.mff.cuni.cz/~kaplicky/pages/pages/2021l/book.pdf

Citation: Gokavarapu C. Asymmetry in Spectral Graph Theory: Harmonic Analysis on Directed Networks via Biorthogonal Bases. Ann Math Phys. 2026;9(1):001-006. Available from: https://dx.doi.org/10.17352/amp.000174

8. Higham NJ. What is a (non) normal matrix? [Internet]. 2020. Available from: https://nhigham.com/2020/11/24/what-is-a-nonnormal-matrix/

9. Norris JR. Markov chains. Cambridge: Cambridge University Press; 1997. Available from: https://cape.fcfm.buap.mx/jdzf/cursos/procesos/libros/norris.pdf

10. Kelly FP. Reversibility and stochastic networks. New York: Wiley; 1979. Available from: https://www.amazon.in/Reversibility-Stochastic-Networks-Cambridge-Mathematical/dp/1107401151

11. Seneta E. Non-negative matrices and Markov chains. 2nd ed. Berlin: Springer; 1981. Available from: https://link.springer.com/book/10.1007/0-387-32792-4

12. Henrici P. Bounds for iterates, inverses, spectral variation and fields of values of non-normal matrices. Numerische Mathematik. 1962;4:24–40. Available from: https://link.springer.com/article/10.1007/BF01386294

13. Lee SL. A practical upper bound for departure from normality. SIAM Journal on Matrix Analysis and Applications. 1995;16:462–468. Available from: https://doi.org/10.1137/S0895479893255184

14. Elsner L, Paardekooper MHC. On measures of nonnormality of matrices. Linear Algebra and its Applications. 1987;92:107–124. Available from: https://doi.org/10.1016/0024-3795(87)90253-9

15. Toh K-C, Trefethen LN. The Kreiss matrix theorem on a general complex domain. SIAM Journal on Matrix Analysis and Applications. 1999;20. Available from: https://doi.org/10.1137/S0895479897324020

16. Ortega A, Frossard P, Kovačević J, Moura JMF, Vandergheynst P. Graph signal processing: Overview, challenges, and applications. Proceedings of the IEEE. 2018;106(5):808–828. Available from: https://ieeexplore.ieee.org/document/8347162

17. Anis A, Gadde A, Ortega A. Efficient sampling set selection for bandlimited graph signals using graph spectral proxies. IEEE Transactions on Signal Processing. 2016. Available from: https://ieeexplore.ieee.org/document/7439829

18. Pesenson I. Sampling in Paley–Wiener spaces on combinatorial graphs. Transactions of the American Mathematical Society. 2008;360:5603–5627. Available from: https://arxiv.org/html/2512.21770v1

19. Marques AG, Segarra S, Mateos G. Signal processing on directed graphs: The role of edge directionality when processing and learning from network data. IEEE Signal Processing Magazine. 2020;37(6):99–116. Available from: https://ieeexplore.ieee.org/document/9244648c

Citation: Gokavarapu C. Asymmetry in Spectral Graph Theory: Harmonic Analysis on Directed Networks via Biorthogonal Bases. Ann Math Phys. 2026;9(1):001-006. Available from: https://dx.doi.org/10.17352/amp.000174